Eur. Phys. J. B (2025)98:178
https://doi.org/10.1140/epjb/s10051-025-01019-9

THE EUROPEAN PHYSICAL JOURNAL B

Research – Statistical and Nonlinear Physics

# Temperature dependence of phase-ordering kinetics of the long-range Ising model with power-law decaying interactions

Ian Filippo Schönherr[a], Fabio Müller[b], and Wolfhard Janke[c]

Institut für Theoretische Physik, Universität Leipzig, IPF 231101, 04081 Leipzig, Germany

Received 2 May 2025 / Accepted 1 August 2025


**Abstract.** We study coarsening in the nonconserved Ising model in $d = 2$ dimensions with long-range interactions decaying as $\sim r^{-(d+\sigma)}$, employing Metropolis Monte Carlo computer simulations based on our recently conceived very efficient predecision scheme. By comparing numerical results between different quench temperatures we confirm the temperature independence of growth laws and show that a sensible choice of temperature may yield longer observation periods in coarsening studies.

## 1 Introduction

The theory of phase-ordering kinetics describes coarsening phenomena in systems that exhibit a phase transition from a disordered high-temperature phase to a symmetry broken ordered phase below the transition temperature $T_c$ [1,2]. In the case of a sudden quench from the disordered into the ordered phase the system will not order instantaneously, instead, ordered domains form that grow with time. This domain growth is characterized by a single characteristic length scale $\ell(t)$, i.e., the average domain size at time $t$. In the nonconserved nearest-neighbor Ising model (NNIM) a growth $\ell(t) \propto t^{1/2}$ is encountered both for quenches to finite quench temperatures $T_q < T_c$ and to $T_q = 0$. This is different in presence of long-range interactions, where the asymptotic behavior of $\ell(t)$ differs between quenches to finite $T_q < T_c$ and $T_q = 0$. In the long-range Ising model (LRIM) in $d = 2$ dimensions (2D) with long-range potentials decaying algebraically as $\sim r^{-(d+\sigma)}$, one finds for zero temperature quenches a power-law behavior of $\ell(t) \propto t^{\alpha}$ with $\alpha \approx 3/4$ independent of $\sigma$ [3]. For very low finite quench temperatures, $\ell(t)$ follows zero temperature dynamics in the preasymptotic regime until finite-$T$ asymptotic behavior is achieved [4], where $\alpha$ is $\sigma$-dependent. For one-dimensional systems, it was shown analytically that the quench temperature influences the crossover point which shifts to ever larger times when approaching $T = 0$, while leaving the eventual asymptotic growth laws unaffected [5].

Previous studies concerning the numerical estimation of the coarsening exponent $\alpha$ were usually conducted by quenches to $T_q = 0.1T_c$ [6–8] with a few exceptions in [4] (where $T_q \leq 0.3T_c$). We want to expand the understanding by directly comparing phase ordering between the well established picture of quenches to low temperatures, i.e., $T_q = 0.1T_c$, and quenches to a yet unexplored high-temperature regime ($T_q = 0.5T_c$) made possible by a new method of simulation.

## 2 Model

The LRIM without an external magnetic field has the Hamiltonian

$$\mathcal{H} = -\sum_i \sum_{j<i} J_{ij} s_i s_j, \qquad J_{ij} = r_{ij}^{-(d+\sigma)}, \tag{1}$$

where $r_{ij} = |\mathbf{r}_i - \mathbf{r}_j|$ is the distance between the sites $i$ and $j$ and $\sigma$ is a parameter controlling the decay of the interaction strength, with spins $s_i, s_j = \pm 1$. Similarly to its short-range counterpart in 2D it exhibits a second-order phase transition from a high-temperature disordered phase to an ordered phase below a $\sigma$-dependent critical temperature $T_c$ [1]. In the case of a sudden quench from the disordered into the ordered phase, the formation and growth of ordered domains of like spins is the characteristic phenomenon. In the NNIM, domain growth is driven by the surface tension of the domain walls and, via the Allen–Cahn equation and the reduction of curvature, it can be shown that $\ell(t) \sim t^{\alpha}$ [1,2], with the growth exponent $\alpha = 1/2$. For the LRIM a prediction has been made comparing energy scalings

[a] e-mail: ianschonherr@gmail.com (corresponding author)
[b] e-mail: fabio.mueller@itp.uni-leipzig.de
[c] e-mail: wolfhard.janke@itp.uni-leipzig.de

Published online: 29 August 2025

giving [9]

$$\ell(t) \propto t^{\alpha} = \begin{cases} t^{1/(1+\sigma)} & \sigma < 1 \\ (t \ln t)^{1/2} & \sigma = 1 \\ t^{1/2} & \sigma > 1 \end{cases}, \tag{2}$$

predicting a $\sigma$-dependent growth exponent in the regime $\sigma \leq 1$ where long-range interactions become the driving force. This growth law has been confirmed numerically by Christiansen et al. [6] for the 2D LRIM using a quench temperature of $T_q = 0.1T_c$.

## 3 Methods

A standard approach for simulation of the Ising model is the Metropolis Monte Carlo method [10,11], where at each time step one proposes a random spin to be flipped with the probability

$$P = \min\{1, \exp(-\beta \Delta E)\}, \tag{3}$$

where $\beta = 1/T$ and

$$\Delta E = E^{\text{new}} - E^{\text{old}} = -\Delta s_i \sum_{j \neq i} J_{ij} s_j \tag{4}$$

with $\Delta s_i = s_i^{\text{new}} - s_i^{\text{old}} = -2s_i^{\text{old}}$ is the energy difference of the system before and after a successful flip. The spin is then flipped if

$$\rho < \exp(-\beta \Delta E) \tag{5}$$

for a (pseudo) random number $\rho \in [0, 1)$. In short-range models each spin only interacts with a small, system-size independent number of spins in its neighborhood and the calculation of $\Delta E$ poses no major challenge. This is in contrast to a fully connected model such as the LRIM, where the computational effort associated with the calculation of $\Delta E$ is directly proportional to the system size $N$. A sweep, consisting of $N$ update attempts for randomly selected spins (the usual choice for one time step), is thus of complexity $O(N^2)$. This makes numerical simulation of phase ordering in long-range models computationally far more expensive than in the short-range case. While for equilibrium studies there exist cluster algorithms that reduce computational complexity as well as the critical slowing down [12,13], for the investigation of dynamical properties we need to rely on update schemes with local dynamics. This is why the theoretical prediction for the growth exponent $\alpha$ of long-range models in Eq. (2) has only recently been confirmed numerically despite the fact that the prediction is already more than three decades old.

Alongside the constant increase in computing power, this was possible due to an improvement upon the standard Metropolis algorithm by the introduction of effective fields $h_i$ which store the energy of each spin $s_i$ [6,14]. The effective fields need only to be updated after an *accepted* update, leaving the computational complexity unaltered, albeit with a much smaller prefactor being inversely proportional to the acceptance rate. The performance gain of the method is thus largest at low temperatures where the acceptance rate is low.

Hence, prior simulations were conducted with a quench temperature of $T_q = 0.1T_c$ where the speedup in comparison to direct sum Metropolis is $\sim 10^3$ [6]. This speedup, however, diminishes for higher quench temperatures, and to efficiently simulate non-equilibrium physics one needs to devise other methods.

In the acceptance criterion (5) one usually computes first $\Delta E$ and then draws the random number $\rho$ [10,11]. In Refs. [15,16] it was noticed that for long-range interacting systems one may profit by reversing this order (in the short-range case, however, this does not pay). This is most obvious by rewriting (5) as

$$E^{\text{th}} = -\frac{\ln \rho}{\beta} > \Delta E \tag{6}$$

which generically defines a threshold energy $E^{\text{th}}$ and shows that an exact computation of $\Delta E$ is not required. Rather, it is only necessary to decide whether $\Delta E$ is *larger or smaller* than $E^{\text{th}}$. This flexibility can be exploited by constructing lower and upper bounds of $\Delta E$,

$$\Delta E_{\min} \leq \Delta E \leq \Delta E_{\max}, \tag{7}$$

which allows one to accept a spin-flip proposal if $\Delta E_{\max} < E^{\text{th}}$ and to reject it if $\Delta E_{\min} \geq E^{\text{th}}$. If no decision is possible, the bounds need to be further refined.

While the reversed order of evaluating the acceptance criterion is not advantageous for short-range models where the exact $\Delta E$ can be obtained with a few operations, for the long-range case this is the key observation for the improvements reported below. In the following we specifically employ the refinement scheme proposed in Ref. [17]. Permuting in Eq. (4) the order of the $j$ indices to $j' \equiv \pi^{(i)}(j) \neq i$ such that the largest couplings $J_{ij'}$ (i.e., shortest distances $r_{ij'}$) appear first in the sum over neighboring spins (see below), the exact $\Delta E$ can be bounded by

$$\Delta E_{\max/\min} = -\Delta s_i \sum_{j=1}^{n} J_{ij'} s_{j'} \pm U(n) \tag{8}$$

where the summation over the first $n$ closest neighbors of $s_i$ is carried out exactly. Noting that $-J_{ij'} \leq J_{ij'} s_{j'} \leq J_{ij'}$ and $-2 \leq -\Delta s_i \leq 2$, the upper and lower bounds of the contribution of the interactions with "far" spins are given by

$$U(n) = 2 \sum_{j=n+1}^{N-1} J_{ij'} = 2 \left( J^{\text{int}} - \sum_{j=1}^{n} J_{ij'} \right) \tag{9}$$

where $J^{\text{int}} \equiv \sum_{j\neq i} J_{ij}$.

For increasing $n$, the bounds $\Delta E_{\text{max/min}}$ get narrower until both approach the exact $\Delta E$ for $n = N - 1$. This predecision scheme hence allows an early decision about the spin-flip proposal once $\Delta E_{\text{max}}(n_{\text{th}}) < E^{\text{th}}$ ("accept") or $\Delta E_{\text{min}}(n_{\text{th}}) \geq E^{\text{th}}$ ("reject"). On average this occurs for $n_{\text{th}} \ll N$, which leads to the significant speedup of this update procedure (which, dynamically, is nevertheless entirely equivalent to the Metropolis algorithm) [17]. For periodic boundary conditions, sorting the indices $j'$ in Eq. (8) can be performed for an arbitrary reference point $i_0$ once at the beginning of the simulation (scaling with system size as $N \log N$), and the corresponding $j'$ for arbitrary $i$ can be computed with few operations during the simulation.

With this method we achieve for $T_q = 0.1T_c$ on a 2D lattice of size $L = 2048$ a speedup of $\sim 3300$ for $\sigma = 0.9$ and $\sim 6800$ for $\sigma = 1.1$ compared to the standard Metropolis update algorithm, which is a factor of $\approx 2$ respectively $\approx 6$ faster than the effective-field method. While at high temperature $T_q = 0.5T_c$ the performance of both methods drops off, the loss is far less significant for the predecision method. We still achieve a reasonable speedup of $\sim 430$ for $\sigma = 0.9$ and $\sim 1400$ for $\sigma = 1.1$ over standard Metropolis while the effective field is at $\sim 30$ for both $\sigma$. The predecision method therefore not only performs well at high $T_q$, it also slightly reduces the computational effort at low $T_q$.

In all our simulations we follow a standard coarsening protocol by starting with an initial random configuration of the system which corresponds to $T = \infty$ and setting the desired quench temperature to $T = T_q$. We implement periodic boundary conditions through the minimum-image convention by surrounding the lattice with imaginary copies. Interactions that exceed the borders of the actual lattice will be treated as interactions with the neighboring copies. If not stated otherwise we use a 2D square lattice of linear size $L = 2048$ and average over 50 independent runs.

## 4 Results

We now want to move on to the ordering kinetics of the LRIM. First, in Fig. 1 we visually compare the coarsening with two different quench temperatures. On the left, snapshots of the LRIM are shown for two different times after a quench to $T_q = 0.1T_c$ (up spins are marked in blue) and on the right to $T_q = 0.5T_c$ (up spins are marked purple). The values for the critical temperature are taken from [18]. We choose $\sigma = 0.9$ which is in the long-range regime where we expect a $\sigma$-dependent growth exponent and $\sigma = 1.1$ where it is equal to the NNIM. Between different temperatures, the only notable difference are thermally excited spins for the higher quench temperature, i.e., single overturned spins inside ordered domains, while the size of the domains does not seem to depend on $T_q$, suggesting a $\sigma$-dependent growth exponent independent of quench temperature, as the growth for $\sigma = 0.9$ appears to be faster in either case.

To verify this visual impression, we now turn to a quantitative assessment of the growth exponent. For that we consider the equal-time two-point correlation function

$$C(r,t) = \langle s_i s_j \rangle, \tag{10}$$

where $\langle \cdots \rangle$ denotes the average over different initial conditions and time evolutions, i.e., different seeds of the pseudo-random number generator.

In Fig. 2 we show an exemplary direct comparison of correlation functions for different $T_q$ with $\sigma = 0.9$. For six different times we compare $C(r,t)$ for $T_q = 0.1T_c$ and $T_q = 0.5T_c$, where the earlier times are shown in (a) and the later ones in (b). Contrary to $T_q = 0.1T_c$ where $C(r,t)$ appears to be smooth, for high $T_q$, upon closer inspection, we notice a jump between $r = 0$ where $C(r,t) = 1$ always and $r = 1$. This can be explained by the fact that the magnetization density inside ordered domains is lower for higher temperatures, directly reflecting the respective concentration of overturned spins in Fig. 1.

For the earlier times in Fig. 2(a) we notice that $C(r,t)$ declines to zero much slower for high $T_q$, such that, despite the initial jump, there is a crossover of correlation functions with different $T_q$. Only for the largest time in Fig. 2(b) it is clear that the correlation at high temperature is smaller for all $r$, as we would expect if a certain amount of spins is randomly flipped due to thermal excitation.

Under the premise of the scaling hypothesis, which states the existence of a single characteristic length scale $\ell(t)$ [1], we expect a collapse of $C(r,t)$ onto a single master curve for all $t$ in the scaling regime if the $r$ axis is rescaled accordingly by a factor $1/\ell(t)$. As is common practice we obtain $\ell(t)$ by setting

$$C(\ell(t),t) = \frac{C(0,t)}{2}. \tag{11}$$

Because of thermally excited spins and the resulting jump of $C(r,t)$ for small $r$ at high $T_q$, a collapse between different $T_q$ cannot be achieved, as can be seen in Fig. 2. Therefore, we treat each quench temperature individually.

This is shown in Fig. 3 for $\sigma = 0.9$ and $T_q = 0.1T_c$ in (a) and $T_q = 0.5T_c$ in (b). Here, the data are plotted over the rescaled axis as described above. In both cases they collapse onto a single master curve. Even though thermally excited spins have a direct influence on the correlation function, they do not contribute to the actual domain size and should not influence the overall scaling behavior.

Another important quantity is the Fourier transform of the correlation function, the structure factor $S(k,t)$. Using the property $C(r,t) = f(r/\ell(t))$ of the correlation function we obtain

$$S(k,t)\ell(t)^{-2} = g(k\ell(t)), \tag{12}$$

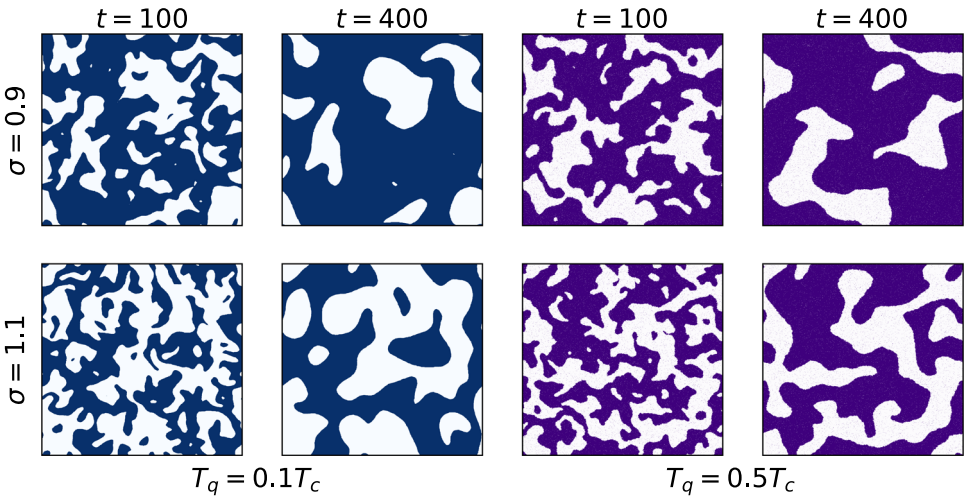


**Fig. 1** Comparison of snapshots with different quench temperatures $T_q$ after a quench to $T_q = 0.1T_c$ (up spins are marked blue) and $T_q = 0.5T_c$ (up spins are marked purple) for different values of $\sigma$ with $L = 1024$. For slower decaying couplings ($\sigma = 0.9$) domains grow faster. We notice a higher density of thermally excited spins for $T_q = 0.5T_c$ while it seemingly vanishes for $T_q = 0.1T_c$. Structure shape, size and growth, however, do not seem to differ between different $T_q$

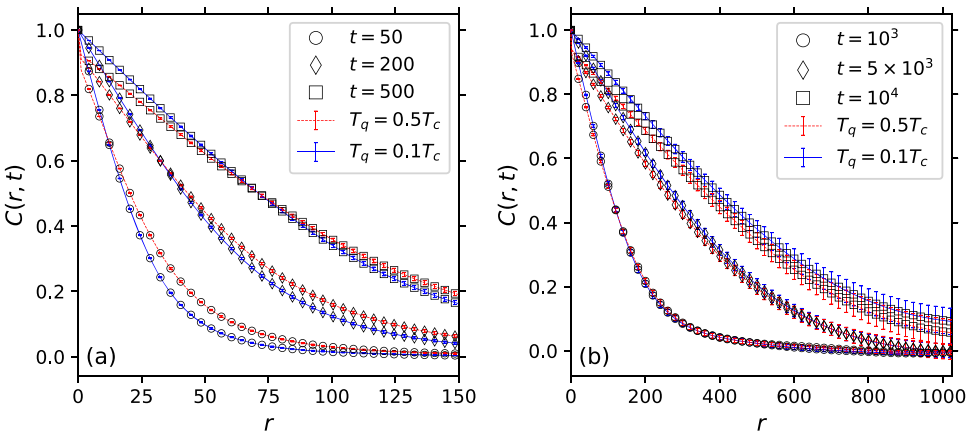


**Fig. 2** Direct comparison of correlation functions with different $T_q$ split into early (**a**) and late (**b**) times for $\sigma = 0.9$

where $f$ and $g$ are arbitrary scaling functions [2]. Again we expect a collapse of the structure factor onto a single master curve by plotting $S(k,t)\ell(t)^{-2}$ over the scaling variable $k\ell(t)$. We show this again for $\sigma = 0.9$ and $T_q = 0.1T_c$ in Fig. 3(c) and $T_q = 0.5T_c$ in Fig. 3(d). For both temperatures we see a convincing collapse as we did for the correlation functions. However, in contrast to the correlation functions where there was little difference between the $T_q$, we notice that the flattening tail end for large $k$ is much more pronounced for $T_q = 0.5T_c$. This can be attributed to the previously discussed jump of the correlation function for small $r$ and high $T_q$. The solid lines indicate Porod's law, i.e., $S(k,t) \propto k^{-3}$ for large $k$ [1]. In both cases we find good agreement, which is important as Porod's law was used to derive Eq. (2) [9]. For $\sigma = 1.1$ we find the same results. The plots are not shown here as they are fairly similar to the ones for $\sigma = 0.9$.

Having confirmed that the known scaling properties for $T_q = 0.1T_c$ carry over to the higher $T_q = 0.5T_c$, i.e., phase ordering in the LRIM is a scaling process independent of quench temperature, we move on to a more quantitative analysis of the length scale $\ell(t)$. In the main plots of Fig. 4 we compare $\ell(t)$ on a double-log scale for both high (red) and low (blue) $T_q$ for $\sigma = 0.9$ in (a) and $\sigma = 1.1$ in (b), respectively. The solid lines correspond to the predicted behavior of Eq. (2). We determine $\ell(t)$ through Eq. (11) and errors have been obtained via Jackknife binning of the correlation functions of individual runs [11], the error bars drawn are two times the standard error of the mean. One immediately notices that in all cases the data follow the prediction for the growth exponent $\alpha$ after an initial preasymptotic regime. For high $T_q$ we observe a noticeably shorter preasymptotic regime resulting in a significantly longer scaling regime until finite-size effects set in at roughly the same $t$ for $\sigma = 0.9$ and quite a bit

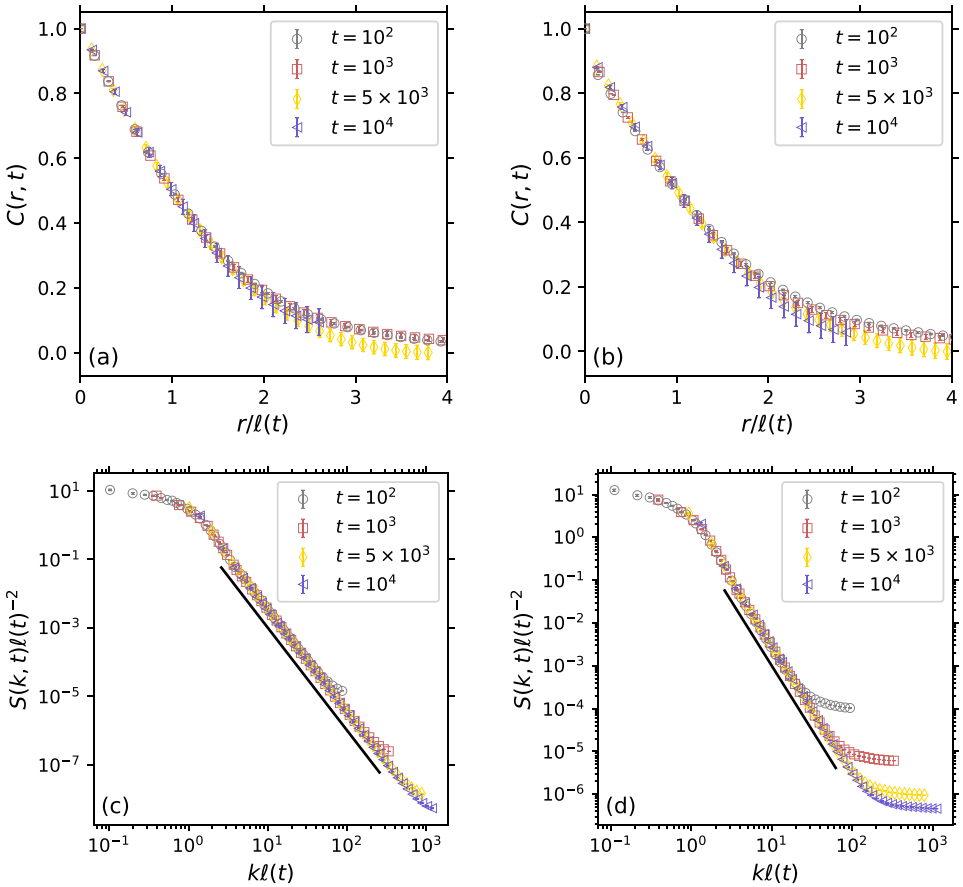


**Fig. 3** Comparison between quench temperatures of the scaled correlation function $C(r,t)$ and structure factor $S(k,t)$ for $\sigma = 0.9$. $C(r,t)$ is plotted over the scaling variable $r/\ell(t)$ for $T_q = 0.1T_c$ in (**a**) and for $T_q = 0.5T_c$ in (**b**). The scaled plots of the structure factor are shown as $S(k,t)\ell(t)^{-2}$ over $k\ell(t)$ for $T_q = 0.1T_c$ in (**c**) and for $T_q = 0.5T_c$ in (**d**). The solid line in (**c**) and (**d**) indicates the Porod tail behavior of $\propto k^{-3}$

earlier for $\sigma = 1.1$ compared to low $T_q$. This follows the trend seen in [4], where $\ell(t)$ for very small but finite $T_q$ follows the zero-temperature behavior. Only for larger $T_q$ the expected power law (2) is recovered after an initial $T_q$-dependent preasymptotic regime. In our case the increase from $0.1T_c$ to $0.5T_c$ more than doubles the scaling regime for both $\sigma$. The effects of quench temperature on the correlation function as discussed above (Fig. 2) are signaled here as well. We see that for large $t$, less correlation yields smaller $\ell(t)$ for high $T_q$. In the early time evolution, the shifting crossing point of the correlation function for different quench temperatures is reflected as a crossover of $\ell(t)$. The insets show the same data divided by the predicted power law as $\ell(t)/t^\alpha$. Assuming $\ell(t) = At^\alpha$ there should be a plateau around the value of the prefactor $A$. The horizontal dashed (solid) lines in the inset correspond to the chosen values of $A$ for the lines in the main plot, the lines are solid in the range of the main plot lines and the believable scaling regime. For both $\sigma$ the data for high $T_q$ show a steep incline in the early stage followed by a long regime where it is nearly flat until for the largest $t$ finite-size effects become visible. For low $T_q$ the initial increase is much slower and the curves start to flatten out over a decade later than those for high $T_q$, resulting in a much shorter flat (scaling) regime before finite-size effects dominate. These observations are consistent with the ones of the main plot and further solidify the picture.

To summarize, we presented numerical results of the LRIM in 2D in a non-equilibrium setting. We have shown that the scaling hypothesis holds true for both choices of quench temperature by collapse of the correlation function and the predicted scaling behavior of $\ell(t) \propto t^\alpha$ (Eq. (2)) is reproduced in a direct comparison of length-scale measurements. We conclude that not only is phase ordering a scaling phenomenon independent of quench temperature for finite $T_q$, but quenches to comparatively higher temperatures further substantiate the growth-law prediction (2) due to an extended scaling regime. We see that the slightly higher computational demand which comes with increasing the temperature leads to a much longer observation period, such

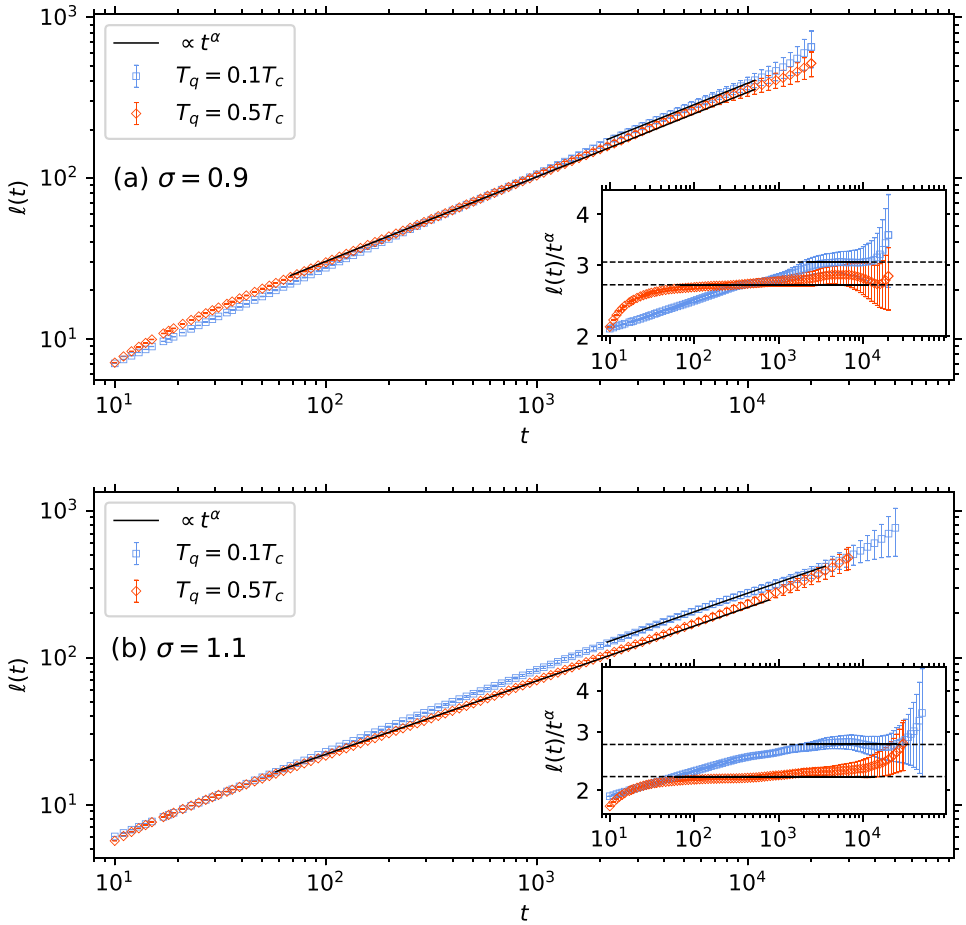


**Fig. 4** The main plots show the time dependence of $\ell(t)$ for both low and high $T_q$ for (**a**) $\sigma = 0.9$ and (**b**) $\sigma = 1.1$. The solid lines correspond to the prediction of Eq. (2) using $\ell(t) = At^\alpha$. In the insets the power-law behavior is divided out as $\ell(t)/t^\alpha$ with the predicted exponents $\alpha$. The values of the corresponding prefactors $A$ used in the main plots are drawn as solid horizontal lines over the same range as in the main plots and as dashed lines over the whole range. Error bars are two times the standard error of the mean

that a careful choice of $T_q$ can be beneficial to more easily unveil asymptotic behavior, especially for models with a more pronounced $T$-dependence of the dynamics.

**Acknowledgement** This project was partially funded by the Deutsch-Französische Hochschule (DFH-UFA) through the Doctoral College "$\mathbb{L}^4$" under Grant No. CDFA-02-07. We further acknowledge support by the Leipzig Graduate School of Natural Sciences "BuildMoNa".

## Author contributions

All authors whose names appear on the submission (1) made substantial contributions to the conception or design of the work; or the acquisition, analysis, or interpretation of data; or the creation of new software used in the work; (2) drafted the work or revised it critically for important intellectual content; (3) approved the version to be published; and (4) agree to be accountable for all aspects of the work in ensuring that questions related to the accuracy or integrity of any part of the work are appropriately investigated and resolved.

**Funding** Open Access funding enabled and organized by Projekt DEAL. This project was partially funded by the Deutsch-Französische Hochschule (DFH-UFA) through the Doctoral College "$\mathbb{L}^4$" under Grant No. CDFA-02-07. We further acknowledge support by the Leipzig Graduate School of Natural Sciences "BuildMoNa".

**Data Availability Statement** The datasets generated during and/or analyzed during the current study are available from the corresponding author on reasonable request. Data will be made available on reasonable request

**Code Availability Statement** Not applicable.

**Declarations**

**Conflict of interest** None.

**Ethics approval and consent to participate** Not applicable.

**Consent for publication** Not applicable.



## References

1. A.J. Bray, Theory of phase-ordering kinetics. Adv. Phys. **51**, 481 (2002). https://doi.org/10.1080/00018730110117433
2. R. Livi, P. Politi, *Nonequilibrium Statistical Physics: A Modern Perspective* (Cambridge University Press, Cambridge, 2017). https://doi.org/10.1017/9781107278974
3. H. Christiansen, S. Majumder, W. Janke, Zero-temperature coarsening in the two-dimensional long-range Ising model. Phys. Rev. E **103**, 052122 (2021). https://doi.org/10.1103/PhysRevE.103.052122
4. R. Agrawal, F. Corberi, E. Lippiello, P. Politi, S. Puri, Kinetics of the two-dimensional long-range Ising model at low temperatures. Phys. Rev. E **103**, 012108 (2021). https://doi.org/10.1103/physreve.103.012108
5. F. Corberi, E. Lippiello, P. Politi, One dimensional phase-ordering in the Ising model with space decaying interactions. J. Stat. Phys. **176**, 510 (2019). https://doi.org/10.1007/s10955-019-02313-4
6. H. Christiansen, S. Majumder, W. Janke, Phase ordering kinetics of the long-range Ising model. Phys. Rev. E **99**, 011301 (2019). https://doi.org/10.1103/physreve.99.011301
7. W. Janke, H. Christiansen, S. Majumder, Coarsening in the long-range Ising model: Metropolis versus Glauber criterion. J. Phys: Conf. Ser. **1163**, 012002 (2019). https://doi.org/10.1088/1742-6596/1163/1/012002
8. W. Janke, H. Christiansen, S. Majumder, The role of magnetization in phase-ordering kinetics of the short-range and long-range Ising model. Eur. Phys. J. Spec. Top. **232**, 1693 (2023). https://doi.org/10.1140/epjs/s11734-023-00882-w
9. A.J. Bray, A.D. Rutenberg, Growth laws for phase ordering. Phys. Rev. E **49**, 27 (1994). https://doi.org/10.1103/physreve.49.r27
10. M.E.J. Newman, G.T. Barkema, *Monte Carlo Methods in Statistical Physics* (Oxford University Press, Oxford, 1999). https://doi.org/10.1093/oso/9780198517962.001.0001
11. D.P. Landau, K. Binder, *A Guide to Monte Carlo Simulations in Statistical Physics* (Cambridge University Press, Cambridge, 2014). https://doi.org/10.1017/cbo9781139696463
12. E. Luijten, H.W.J. Blöte, Monte Carlo method for spin models with long-range interactions. Int. J. Mod. Phys. C **06**, 359 (1995). https://doi.org/10.1142/s0129183195000265
13. K. Fukui, S. Todo, Order-$N$ cluster Monte Carlo method for spin systems with long-range interactions. J. Comput. Phys. **228**, 2629 (2009). https://doi.org/10.1016/j.jcp.2008.12.022
14. A. Hucht, A. Moschel, K. Usadel, Monte-Carlo study of the reorientation transition in Heisenberg models with dipole interactions, J. Magn. Magn. Mater. **148**, 32 (1995). https://doi.org/10.1016/0304-8853(95)00137-9
15. S. Schnabel, W. Janke, Accelerating polymer simulation by means of tree data-structures and a parsimonious Metropolis algorithm. Comput. Phys. Commun. **256**, 107414 (2020). https://doi.org/10.1016/j.cpc.2020.107414
16. F. Müller, H. Christiansen, S. Schnabel, W. Janke, Fast, hierarchical, and adaptive algorithm for Metropolis Monte Carlo simulations of long-range interacting systems. Phys. Rev. X **13**, 031006 (2023). https://doi.org/10.1103/PhysRevX.13.031006
17. F. Müller, W. Janke, e-print arXiv:2508.09775 [cond-mat.stat-mech] (2025). https://doi.org/10.48550/arXiv.2508.09775
18. T. Horita, H. Suwa, S. Todo, Upper and lower critical decay exponents of Ising ferromagnets with long-range interaction. Phys. Rev. E **95**, 012143 (2017). https://doi.org/10.1103/PhysRevE.95.012143